HHS Public Access

Author manuscript

Gastroenterology. Author manuscript; available in PMC 2015 May 04.

Published in final edited form as:

Gastroenterology. 2008 December ; 135(6): 1993–2002. doi:10.1053/j.gastro.2008.08.053.

CD44 Deficiency Attenuates Chronic Murine Ileitis

COLM B. COLLINS[*], **JOHNSON HO**[‡], **THEODORE E. WILSON**[*], **JOSHUA D. WERMERS**[*], **JOSÉ L. TLAXCA**[§], **MICHAEL B. LAWRENCE**[§], **MICHAEL SOLGA**[||], **JOANNE LANNIGAN**[||], and **JESÚS RIVERA–NIEVES**[*]

[*]Mucosal Inflammation Program, Division of Gastroenterology, University of Colorado Health Sciences Center, Denver, Colorado

[‡]Digestive Health Center of Excellence, University of Virginia Health Sciences Center, Charlottesville, Virginia

[§]Department of Biomedical Engineering, University of Virginia Health Sciences Center, Charlottesville, Virginia

[||]Flow Cytometry Core Facility, University of Virginia Health Sciences Center, Charlottesville, Virginia

Abstract

Background & Aims—Lymphocyte recruitment to sites of inflammation requires the sequential engagement of adhesion molecules and chemokine receptors. In the current studies we analyzed the role of CD44 for the development of chronic small-intestinal inflammatory infiltrates in vivo.

Methods—By using a tumor necrosis factor (TNF)-driven model of chronic ileitis (ie, B6.129P-$TNF^{\Delta AU\text{-rich element [ARE]}}$) that recapitulates many features of Crohn's disease, we noticed dynamic changes in the expression and functional state of CD44 and its ligand hyaluronan via enzyme-linked immunosorbent assay, real-time reverse-transcription polymerase chain reaction, immunohistochemistry, and flow cytometry. In addition, we assessed the role of lymphocyte populations during induction of ileitis through adoptive transfer studies, and generated CD44-deficient TNFΔARE mice to assess the role of CD44 for development of ileitis.

Results—Soluble hyaluronan levels and expression of hyaluronan synthase-1 were increased in TNFΔARE mice. This coincided with increased expression of CD44 (including variant 7) and reactivity towards hyaluronan on $CD4^+$ T cells. CD44 was spatially co-localized with the gut-homing integrin $\alpha_4\beta_7$, spatially linking lymphocyte rolling with arrest. These cells had an effector phenotype because they lacked L-selectin and a higher proportion in diseased mice produced TNF and interleukin-2 compared with wild-type littermates. Lastly, $CD4^+$ but not $CD8^+$ T cells conferred ileitis to $RAG^{-/-}$ recipients and deficiency of one or both alleles of the CD44 gene resulted in attenuation of the severity of ileitis in TNFΔARE mice.

Address reprint requests to: Jesús Rivera-Nieves, MD, Mucosal Inflammation Program, University of Colorado Health Sciences Center, BRB, Room 742A, 4200 E. 9th Avenue, B146, Denver, Colorado 80206. jesus.rivera-nieves@uchsc.edu; fax: (303) 315-5711.

The authors disclose the following: Supported by US Public Health Service/National Institutes of Health grants DK067254 and DK073280 (J. R.-N.) and by the University of Virginia Silvio Conte Digestive Health Research Center (grant DK56703).

Conclusions—Our findings support an important role of CD44 expressed by $CD4^+$ and $CD8^+$ for development of ileitis mediated by TNF overproduction.

Ulcerative colitis (UC) is strictly a colonic disease, whereas Crohn's disease (CD) involves the small bowel in two thirds of patients.[1] One explanation for this difference is that the recirculating effector/memory cell pool expresses distinct repertoires of adhesion molecules and chemokine receptors that drive differential traffic between the small and large bowels.[2] Our knowledge of the specific molecules that mediate small-intestinal homing during chronic ileitis is limited, in part because of the lack of animal models that develop chronic inflammation localized to the terminal ileum.[3]

The tumor necrosis factor (TNF)ΔAU-rich element (ARE) model is 1 of only 2 mouse inflammatory bowel disease (IBD) models that develop chronic inflammation localized to the ileum, reminiscent of human CD in its histologic features and the pivotal role played by TNF in its pathogenesis. Targeted deletion of 69 base pairs within the AU-rich region of the TNF gene resulted in increased messenger RNA (mRNA) stability, increased TNF protein synthesis, and systemic levels of TNF. In addition, these mice develop deforming arthritis, similar to human rheumatoid arthritis, in both heterozygous and homozygous mice.[4] Interestingly, both CD and rheumatoid arthritis respond therapeutically to TNF antagonists (eg, infliximab, adalimumab, and certolizumab), supporting the relevance of this model for the investigation of pathogenic mechanisms that mediate the human diseases.[5]

TNF overproduction increases the expression of CD44 on $CD8^+$ lymphocytes;[6] however, within the $CD8^+$ T-cell population there are both effector and regulatory arms, defined by the presence or absence of CD44 or CD103 on the cell surface.[7] In the present study we investigated whether the inflammatory process affects the levels of hyaluronan (HA) or the enzymes that mediate its synthesis (ie, hyaluronan synthases [HAS]). We analyzed the proportion of $CD4^+$ T cells that express CD44 during early and established disease and examined potential integrins that support arrest in CD44-expressing lymphocytes. We additionally investigated the capacity of $CD4^+$ and $CD8^+$ T cells to adoptively transfer ileitis to $RAG^{-/-}$ recipients and assessed the functional role of CD44 in ileitis by developing TNFΔARE mice deficient for CD44 on the cell surface.

Materials and Methods

Mice

The B6.129S-Tnf^{tm2Gkl}/Jarn strain (MGI: 3720980) was generated by continuous backcrosses between $TNF^{\Delta ARE}$ mice on mixed genetic background (ie, C57BL6 and 129S6)[4] to C57BL6/J mice as previously described.[7] Mice were kept under specific pathogen-free conditions. All progeny were either heterozygous ($TNF^{\Delta ARE/+}$, TNFΔARE) or carried no mutated alleles, wild-type (WT). The latter were used as the noninflamed controls. CD44-, integrin β_7-, and L-selectin–deficient mice on the C57BL6/J background were obtained from Jackson Laboratories (Bar Harbor, ME). All animal procedures were approved by the institutional committees for animal use of the Universities of Virginia and Colorado.

Detection of Serum Hyaluronan Concentration by Enzyme-Linked Immunosorbent Assay

Serum from 30-week-old TNFΔARE and WT littermates was separated by centrifugation from red blood cells, snap-frozen in liquid nitrogen, and stored at −80°C. Serum hyaluronan levels were determined by enzyme-linked immunosorbent assay as per the manufacturer's instructions (Corgenix, Westminster, CO).

Tissue Collection and Histologic Analyses

The distal ilea (10 cm) were fixed in 10% buffered formalin, embedded, cut into 3- to 5-μm sections, and stained with H&E. Histologic assessment of ileal inflammation was performed using a standardized semiquantitative scoring system, as described previously.[8]

Immunohistochemistry

Terminal ilea were snap-frozen and sectioned (5 μm) on a cryostat (Microm HM505N, Walldorf, Germany), incubated with biotinylated hyaluronan binding protein (US Biological, Swampscott, MA) in the presence or absence of soluble hyaluronan (Sigma, St. Louis, MO), which served as a specificity control, followed by incubation with horseradish-peroxidase–labeled streptavidin (BD Biosciences, San José, CA).

Real-Time Reverse-Transcription Polymerase Chain Reaction

Total RNA was isolated from homogenized ileal tissue using the RNeasy Mini Kit (Qiagen, Valencia, CA) and converted to complementary DNA (cDNA) with the GeneAmp RNA polymerase chain reaction (PCR) kit (Applied Biosystems, Foster City, CA) using random hexamers (0.75 μg of total RNA, final reaction volume 20 μL). cDNA was quantified by real-time PCR using an ABI PRISM 7000 Sequence Detection System (Applied Biosystems). Primers (1.25 μL TaqMan Gene Expression Assays: HAS-1, mm00468496_m1, HAS-2, mm00515089_m1, HAS-3, mm00515091_m1; Applied Biosystems), 4 μL of first-strand cDNA, 12.5 μL of TaqMan 2× PCR master mix, and 7.25 μL of water were mixed together for each reaction. Each PCR reaction was performed in triplicate. Thermocycling conditions for the targets were as follows: 50°C for 2 minutes (iTaq DNA polymerase activation), 95°C for 10 minutes and 40 cycles of 95°C for 15 seconds, and 60°C for 1 minute. In each sample, 18S RNA expression was measured as endogenous control. The reaction volume (10 μL) for CD44v7 contained iQ SYBR Green PCR Supermix (Bio-rad, Hercules, CA), primer pairs (forward 5′CAGCCTGT-TGGGTTGGTATT 3, reverse 5′CAGACTCAGGAGCCCACAAC 3′), and cDNA template. Samples were run in duplicate for 1 cycle (95°C for 10 s) followed by 40 cycles (95°C for 15 s, 60°C for 1 min). Fluorescence was measured after each cycle. The ratio of mRNA expression was calculated by the ΔΔcycle threshold method (User Bulletin no. 2; Applied Biosystems).

Lymphocyte Isolation

Single-cell suspensions were obtained by passing the spleen or mesenteric lymph node (MLN) through a 100-μm cell-strainer. Lamina propria mononuclear cells were isolated as previously described.[9] Red blood cells were lysed by a 15-minute incubation in ammonium chloride lysing reagent (BD PharM Lyse; BD Biosciences).

Adhesion Assay Under Flow

Freshly isolated cells isolated from MLN were cultured in complete medium (RPMI with 10% fetal calf serum, 2 mmol/L L-glutamine, 100 U penicillin, 100 mg/mL streptomycin, 10 mmol/L HEPES, 1 mmol/L sodium pyruvate, nonessential amino acids, 1×10^5 M2ME) in the presence of anti-CD3 (5 μL/mL) for 24 hours at 37°C. Polystyrene dishes were coated overnight with 500 μL of 2.5 mg/mL soluble rooster comb hyaluronan (Sigma). Nonspecific adhesion sites were blocked with 0.5% Tween-20 in Hank's Balanced Salt Solution (HBBS) for 1 hour. Cell suspensions (2×10^6 cells/mL) were drawn into the chamber at 37°C using a syringe pump (Harvard Apparatus, South Natick, MA). Physiologic flow conditions were produced in a 35-mm parallel flow chamber (Glyco Tech, Rockville, MD) at a shear stress of 2 dyn/cm^2. Equilibrium was attained and interactions were monitored using an inverted phase-contrast microscope (Diaphot–TMD; Nikon, Garden City, NY) at 10× magnification. Rolling cells were counted in 8 or more fields of view, changing fields every 25 seconds.

Flow Cytometry and Intracellular Cytokine Staining

Cells from indicated compartments were incubated with antibodies against the following: mouse CD4 (GK1.5) for gating, CD44 (IM7), L-selectin (MEL-14), CD103 (M290), and integrin β_7 (M293; BD Biosciences) or their respective isotype controls. Additional controls included cells isolated from respective organs of mice deficient for CD44, L-selectin, and integrin β_7. Separate cytokine staining was performed using the BD Cytofix/Cytoperm kit as per the manufacturer's instructions (BD Biosciences). Cells were fixed with 2% paraformaldehyde and 4–5 color analyses were performed using the FACS Calibur system (Beckton–Dickinson Immunocytometry Systems, San José, CA, modified by Cytek Development, Fremont, CA). Further analyses were performed using FLOWJo software (Tree Star Inc, Ashland, OR).

Multispectral Imaging Flow Cytometry

Cells isolated from MLN of TNFΔARE mice were incubated with anti-integrin antibodies for 15 minutes at 37°C to allow for capping of the integrins, washed, re-suspended in staining buffer, incubated with antibodies against CD44 (IM7), integrin CD103 (M290), or integrin $\beta_4\beta_7$ (DATK32) for 20 minutes at 4°C, then washed and fixed with 2% paraformaldehyde. Images (10,000 events) were acquired on the Imagestream imaging cytometer (Amnis, Seattle, WA). Unstained cells and cells stained with a single antibody/fluorophore combination were acquired without bright field illumination and used for compensation. Spectral compensation and data analysis were performed using the IDEAS image analysis software package (Amnis).

The similarity bright detail score (SBDS) was calculated in a 3-step process: (1) determination of the opening residue image for each channel image; (2) calculation of a non-mean normalized Pearson correlation coefficient; and (3) log transformation of the correlation coefficient to give roughly Gaussian distributions, the mean of which is the SBDS.[10,11] Poorly colocalized events have SBDS values of 1 to 2, whereas colocalized events have SBDS values of 3 or greater.

Induction of Ileitis by Transfer of T-Cell Subsets to Recombination-Activating Gene$^{-/-}$ Mice

$CD4^+$ T cells from spleen of TNFΔARE mice were isolated by positive selection with anti-mouse CD4 microbeads as per the manufacturer's instructions (Miltenyi Biotec, Auburn, CA). Preliminary studies, which compared the ability of positively or negatively selected $CD4^+$ to transfer ileitis, showed that the selection method did not affect the severity or time course of the resultant disease in recombination-activating gene $(RAG)^{-/-}$ recipients. The flow-through then was stained with fluorescein isothiocyanate–labeled anti-mouse CD8 antibody, phycoerythrin-labeled rat anti-mouse CD103 and APC-labeled rat anti-mouse CD44. Unfractionated $CD8^+$, $CD8^+/CD44^+$, and $CD8^+/CD103^+$ subsets were separated using a fluorescence-activated cell sorter Vantage SE Diva system (BD Biosciences). T-cell fractions (≥97% pure) (5×10^5) were suspended in 500 μL of phosphate-buffered saline and injected intraperitoneally into 6-week-old female $RAG^{-/-}$ recipients. Their ilea were harvested after 6 weeks and the severity of inflammation was assessed as described.[8]

Statistics

Statistical analyses were performed using the 2-tailed Student *t* test or 2-way analysis of variance. Data were expressed as mean ± standard error of the mean (SEM). Statistical significance was set at a *P* value of less than .05.

Results

Increased Expression of Hyaluronan and Hyaluronan Synthase-1 in TNFΔARE Mice

We compared the levels of hyaluronan in serum, the expression of hyaluronan synthases, and the reactivity of hyaluronan binding protein within the terminal ileum. Levels of soluble hyaluronan were increased significantly in 30-week-old TNFΔARE mice with ileitis compared with WT mice (822 ± 121 vs 410 ± 51 ng/mL; $P < .01$; Figure 1*A*).

To try to identify the enzyme(s) responsible for increased hyaluronan levels, we assessed the expression of hyaluronan synthases 1–3 (HAS-1, -2, and -3) (Figure 1*B*) in ileum. Expression of HAS-1, but not HAS-2 or -3, was up-regulated significantly during peak and late disease in 10- and 30-week-old mice compared with WT mice (Figure 1*B*), because the severity of ileitis progressively worsens (Figure 1*C*). By contrast, HAS-3 appeared to decrease during late disease, yet the differences between WT and TNFΔARE did not reach statistical significance.

Hyaluronan Is Expressed on Crypt Cells and Infiltrating Leukocytes in the Ileum of TNFΔARE Mice

As shown in Figure 1*D*, hyaluronan localized predominantly to the crypt regions (Figure 1*D*, *inset middle panel*) and to the surface of infiltrating leukocytes, which were more numerous in inflamed ileum of TNFΔARE mice (*middle panel*) than in WT mice (*top panel*). Pre-incubation of hyaluronan binding protein with soluble hyaluronan confirmed signal specificity (Figure 1*D*, *bottom*).

Increased Reactivity and Rolling Flux Fractions by CD4+ T Cells in TNFΔARE Mice

To determine whether chronic inflammation influenced the functional state of CD44 in vivo, we assayed the ability of $CD4^+$ T cells freshly isolated from MLN of WT mice and TNFΔARE mice to bind fluorescent hyaluronan. Significantly more T cells from TNFΔARE mice bound fluorescent hyaluronan, both within the $CD44^{high}$ (45 ± 5 vs 31 ± 2; $P < .01$) and within the $CD44^{low}$ (23 ± 3 vs 7 ± 4; $P < .01$; Figure 2*A* and *B*). Flow chamber rolling studies confirmed that a higher percentage of cells from TNFΔARE mice show rolling interactions on a hyaluronan-coated flow chamber compared with WT controls (53.2% ± 7% increase; Figure 2*C*).

Percentage of $CD4^+/CD44^{high}$ T Cells Increased in TNFΔARE Mice

We then examined the surface expression of CD44 on $CD4^+$ (Figure 3) and $CD19^+$ cells (data not shown) from spleen, MLN, and lamina propria of TNFΔARE mice (Figure 3, *white histograms*) during early (4 week) and late disease (≥20 week), compared with WT littermates (*gray histograms*). Corresponding isotype antibodies (mean flourescence intensity < 10^1, not shown) and lymphocytes isolated from CD44-deficient mice were used as controls (Figure 3, *discontinuous histograms*). At 4 weeks of age, when there is no histologic evidence of ileitis, the intensity of expression in $CD4^+$ cells isolated from spleen, MLN, and lamina propria of WT and TNFΔARE mice were similar. However, by 20 weeks of age, when the ileitis is fully established, there was an increase in the $CD44^{high}$ population within the $CD4^+$ T cells from the spleen (43% vs 22%), MLN (26% vs 16%), and lamina propria (60% vs 37%). No significant changes were observed in the $CD19^+$ cells from inflamed and noninflamed mice, although the mean fluorescence intensities were shifted to the right by 20 weeks of age or older, consistent with an age-related increase in expression (data not shown).

When the absolute numbers of $CD44^{high}$ cells were calculated by correcting the percentages of expression against the cellularity of spleen and MLN, an increase in the frequency of $CD4^+$ $CD44^{high}$ cells occurs in MLN of 20-week-old and older TNFΔARE mice (WT = 2.7 ± 0.6 × 10^6 vs TNFΔARE = 6.8 ± 0.8 × 10^6; $P < .01$). Within the spleen the differences did not reach statistical significance (WT = 15.4 ± 2.4 × 10^6 vs TNFΔARE = 16.8 ± 3.3 × 10^6) because the cellularity of spleen decreases during advanced disease.

Expression of CD44 Variant Exon v7 mRNA Is Increased in Inflamed Ileum of TNFΔARE Mice

The mRNA levels for variant exon 7 (CD44v7) were determined in the inflamed total ileum and noninflamed colonic tissues from 20-week-old and older TNFΔARE mice (*white bars*) and WT (*gray bars*) using real-time reverse-transcription PCR, normalized to the glyceraldehyde-3-phosphate dehydrogenase mRNA internal control in each sample (Figure 3*D*). The expression of CD44v7 mRNA was significantly higher in the inflamed ilea of TNFΔARE mice compared with that of normal WT controls (*gray bars*). By contrast, there was no difference in the expression within uninflamed colonic tissues of TNFΔARE and WT mice, supporting induction within the ileum by inflammatory mediators.

Most CD44+ T Cells Co-Express β7 Integrins, Which Colocalize With CD44 on the Lymphocyte Surface

We investigated whether the expanded $CD44^+$ subset in TNFΔARE mice co-expressed β_7 integrins and whether the gut-homing β_7^+ T cells bind hyaluronan (Figure 4*A* and *B*). Most $CD4^+$ T cells in MLN of WT and TNFΔARE mice expressed intermediate levels of β_7 integrins (MFI, ~10^2) and these $\beta_7^{intermediate}$ cells comprised most of the cells that bind hyaluronan. Because β_7 pairs with either integrins α_4 or CD103, we investigated which of the α subunits (ie, α_4, CD103) is co-expressed on the surface of CD44-expressing cells by probing cells with an antibody that recognizes the $\alpha_4\beta_7$ heterodimer (ie, clone DATK32) or CD103. Binding was analyzed using multi-spectral imaging flow cytometry. The fluorescent images obtained (Figure 4*C*) suggested colocalization of CD44 and $\alpha_4\beta_7$ on the cell surface. Data then were compared to determine the degree of colocalization (ie, high SBDS).[10] The median SBDS between $\alpha_4\beta_7$ and CD44 was 3.3 ± 0.5 (minimum, 2; maximum, 4.3), whereas between CD103 and CD44 was 0.5 ± 0.4 (minimum, 0.2; maximum, 2.2) (Figure 4*D*). The high score (≥3) suggests that CD44 was not only co-expressed with $\alpha_4\beta_7$, but also spatially colocalized on the cell surface. By contrast, the low median SBDS between CD103 and CD44 excluded colocalization.

Expanded CD4+ Population Show Effector/Memory Phenotype

We evaluated the phenotype of the $CD4^+$ T-cell population from the spleen and MLN of TNFΔARE and WT controls. The expanded CD44 population in TNFΔARE mice showed predominance of an effector memory phenotype ($CD44^{high}$/L-$selectin^{low}$, Figure 5). The percentages of effector $CD4^+$ cells increased in the spleen (WT = 19% ± 8% vs TNFΔARE = 30% ± 7%; $P < .01$) and in the MLN (WT = 15% ± 3% vs TNFΔARE = 31% ± 9%; $P < .01$) of TNFΔARE mice.

Interleukin-2 and TNF Production Increases in CD4+/CD44high T Cells From TNFΔARE Mice

To begin to understand the role of the $CD4^+/CD44^+$ subset in the disease process we assessed its cytokine profile. We found an increase in number of $CD44^{high}$ T cells that produce TNF in spleen (27% vs 18%) and MLN (16% vs 9%) (Figure 6, *left panels*). Similarly, the number of $CD44^{high}$ T cells that produce interleukin-2 increased in spleen (18% vs 13%) and MLN (12% vs 7%) of TNFΔARE mice compared with WT littermates (Figure 6, *right panels*).

CD4+ T Cells Adoptively Transfer Ileitis to RAG−/− Mice

To assess the relative contribution of T-cell populations to intestinal inflammation, we adoptively transferred unfractionated $CD4^+$ or $CD8^+$ T cells isolated from spleen and MLN of TNFΔARE mice into immunodeficient $RAG^{-/-}$ mice. Transfer of $CD4^+$ but not $CD8^+$ T cells induced ileitis in $RAG^{-/-}$ mice (Figure 7). We recently described that the $CD8^+/CD103^+$ subset contains regulatory T cells,[7] thus we fractionated the 2 major CD8+ subsets and transferred them individually into RAG−/− mice. $CD8^+/CD44^+$ T cells were unable to induce ileitis even when the regulatory $CD8^+/CD103^+$ T-cell subset was depleted.[7] These findings suggest a critical effector role for the $CD4^+$ T-cell population for the induction of ileitis.

CD44 Deficiency Results in Dose-Dependent Attenuation of Ileitis in TNFΔARE Mice

To assess the role of CD44 in vivo in the pathogenesis of ileitis, we generated TNFΔARE mice deficient for one or both alleles of the CD44 gene (Figure 8). Blinded histologic examination of the severity of ileitis in the resultant progeny revealed considerable differences between inflammatory indices in ileal tissues from CD44-sufficient (+/+) mice (8.4 ± 1.2, n = 35) to CD44 heterozygous (+/−) mice (5.4 ± 1.8; $P < 0.01$; n = 20) and CD44-deficient (−/−) TNFΔARE mice (1.2 ± 0.7; $P < .0001$; n = 16). Partial or complete deficiency for CD44 in sibling mice that did not carry the TNFΔARE allele did not develop ileitis or colitis (not shown).

Discussion

A prior study in the TNFΔARE mouse model of CD showed that the CD8/CD44^{high} T-cell population played an important role in disease development.[6] The current study extends those observations to additionally show that CD4/CD44^{+} effectors also are important players. These CD4^{+} T cells have an effector surface phenotype, show enhanced reactivity to HA, produced TNF and interleukin-2, and were required for the induction of ileitis in RAG−/− mice. We additionally show that the synthesis of the CD44 ligand hyaluronan is increased locally and in serum, and that the HAS-1 enzyme is also increased in ileum of TNFΔARE mice. This increase is associated with increased expression of CD44 on the CD4^{+}, which spatially colocalizes with integrin $\alpha_4\beta_7$ on the cell surface.

Increased HA has been reported in human IBD.[12] However, the specific HAS isoform responsible for increased HA in the intestine has not been described. In TNFΔARE mice the expression of HAS-1 correlated with progression of disease, suggesting that this enzyme may play a role during the progression of the disease. This is consistent with data from synoviocytes in which proinflammatory stimuli such as interleukin-1β and prostaglandin E_2 induced expression of HAS-1.[13,14] Another cytokine with a dual role for the expression of HAS is transforming growth factor-β, which stimulates HAS-1 yet inhibits HAS-3.[15] We recently described a regulatory T-cell population that produces transforming growth factor-β[7] and may in part explain the trend towards decreased expression of HAS-3 observed during late disease.

The localization of HA to leukocytes infiltrating the small-intestinal lamina propria is in agreement with a recent study.[16] It is proposed that HA binding protein has increased reactivity towards HA bound to CD44, more than to free hyaluronate. Because crypt cells also express CD44, these cells were also reactive towards HA binding protein, similar to what was reported previously in the large intestine.[17] To a lesser degree we also observed reactivity within the muscularis propria, particularly in inflamed TNFΔARE mice. This is in agreement with a prior study in which viral infection increased HA expression by smooth muscle cells.[18] CD44/hyaluronan interactions thus may in part mediate the transmural migration of effector (CD44^{+}) lymphocytes in these mice, a shared feature of this model and CD.

Prior studies have shown that the total surface expression of CD44 does not necessarily correlate with the ability of the molecule to bind HA.[19] Indeed, although many cell lines

constitutively express activated CD44, its functional state in vivo is tightly regulated.[20] This is not surprising because CD44–HA interactions are ubiquitously relevant for cellular processes. We show that the fraction of cells that carried CD44 in an activated state was higher in TNFΔARE than WT littermates, supporting modulation of the reactivity of CD44 by inflammatory mediators in vivo.

CD44 is widely expressed on hematopoietic cells, but also on endothelium, reflecting its versatility as an adhesion molecule.[21] Although many alternatively spliced isoforms have been described (CD44v1–10), the most common is the hematopoietic or standard (CD44H or s), which is the major form expressed on leukocytes.[22] A prior study showed that the expression of CD44 was greatly increased within the $CD8^+$ population from spleen of TNFΔARE mice.[6] Yet, when we additionally analyzed the expression of CD44 on cells originating from the MLN, we detected expansion of the $CD44^{high}$ subset also within the $CD4^+$. Because this expansion is observed in mice at the peak of the disease rather than during early disease and is not present in age-matched WT littermates, these changes are attributable to the chronic inflammatory process, supporting a role for CD44-expressing $CD4^+$ T cells in chronic ileitis. Our findings are in agreement with work by other groups in which Th-1- and Th-2-polarized $CD4^+$ T cells use CD44 to roll on HA.[16,23]

Among the CD44 isoforms, variant v7 is expressed by Th-1–polarized T cells and macrophages. Immunoblockade of this variant improved trinitrobenzene sulphonic acid colitis[24] and CD44v6/v7-deficient mice were protected from trinitrobenzene sulfonic acid. In agreement, CD44v6/v7/interleukin-10 double-deficient mice were protected from colitis.[25] In our studies, increased expression of CD44v7 in the inflamed ileum, but not in the normal colon, of TNFΔARE mice suggests that this variant may additionally be important in ileitis.

A growing body of evidence suggests that there may be overlap in the function of molecules initially believed to mediate exclusively the early steps of the adhesion cascade (ie, tethering/rolling) with the later steps (ie, firm adhesion). Indeed, Nandi et al[26] have shown that there is physical association between CD44 and $\alpha_4\beta_1$ (VLA-4). This novel finding spatially links the molecules involved in rolling and arrest on the surface of the migrating cell in an unprecedented manner.[27] An association between CD44 and the $\alpha_4\beta_7$ integrin has not been described. Multispectral imaging flow cytometry suggested that there is a similar physical association between CD44 and $\beta_4\beta_7$, but not between CD44 and CD103, the expression of which appear to be mutually exclusive. Prior studies have suggested that $\alpha_4\beta_1$ and $\alpha_4\beta_7$ integrin not only mediate arrest, but also the initial tethering and rolling interactions.[28] Our findings allow us to propose that the foundation for those prior observations might have been based on the close physical association between CD44 with any of the α_4 integrins: $\alpha_4\beta_1$ in the periphery or $\alpha_4\beta_7$ in the intestine. Thus, molecules involved during early and late stages of the adhesion cascade appear to be physically co-localized on the cell surface.

Further analyses revealed that the $CD44^{high}$ cells within the $CD4^+$ population lacked L-selectin, indicative of an effector memory subset ($CD44^{high}$/L-$selectin^{low}$), which recirculate to inflammatory sites while limiting their traffic through secondary lymphoid organs.[29] The

CD8/CD44^{high} T-cell population plays an important role in disease development in TNFΔARE mice.[6] In this study we show that the CD4^{+}, which included CD44^{intermediates} and CD44^{high}, but not the CD8^{+}, T cells from TNFΔARE mice adoptively transferred ileitis into immunodeficient RAG$^{-/-}$ mice, supporting a role for the CD4^{+} cells during induction of ileitis.

A role for CD44 in ileitis was highlighted further by the finding that decreased density of CD44 on the cell surface correlated with the level of attenuation of ileitis in TNFΔARE mice, suggesting that the effect likely is related to an important role for this molecule for the trafficking of pathogenic leukocytes to the ileum. Although the CD8^{+} T cells originally were thought to be the critical effectors in ileitis of TNFΔARE mice based on the attenuating effect of β2-microglobulin deficiency on the severity of ileitis, our studies additionally suggest that CD4^{+}/CD44^{+} T cells also represent an important effector subset for the development of the disease. CD44 thus may be a relevant therapeutic target in IBD.

Acknowledgments

The authors thank Sharon Hoang, Anthony Bruce, Oscar Castañón-Cervantes, and Megan R. Ferguson for technical assistance.

Abbreviations used in this paper

HA	hyaluronan
HAS	hyaluronan synthase
MFI	mean fluorescence intensity
MLN	mesenteric lymph node
PCR	polymerase chain reaction
SBDS	similarity bright detail quantification
SEM	standard error of the mean
TNF	tumor necrosis factor
WT	wild type

References

1. Fiocchi C. Inflammatory bowel disease: etiology and pathogenesis. Gastroenterology. 1998; 115:182–205. [PubMed: 9649475]
2. Kunkel EJ, Butcher EC. Chemokines and the tissue-specific migration of lymphocytes. Immunity. 2002; 16:1–4. [PubMed: 11825560]
3. Strober W, Fuss IJ, Blumberg RS. The immunology of mucosal models of inflammation. Annu Rev Immunol. 2002; 20:495–549. [PubMed: 11861611]
4. Kontoyiannis D, Pasparakis M, Pizarro TT, et al. Impaired on/off regulation of TNF biosynthesis in mice lacking TNF AU-rich elements: implications for joint and gut-associated immunopathologies. Immunity. 1999; 10:387–398. [PubMed: 10204494]
5. Sandborn WJ, Targan SR. Biologic therapy of inflammatory bowel disease. Gastroenterology. 2002; 122:1592–1608. [PubMed: 12016425]

6. Kontoyiannis D, Boulougouris G, Manoloukos M, et al. Genetic dissection of the cellular pathways and signaling mechanisms in modeled tumor necrosis factor-induced Crohn's-like inflammatory bowel disease. J Exp Med. 2002; 196:1563–1574. [PubMed: 12486099]
7. Ho J, Kurtz CC, Naganuma M, et al. A CD8+/CD103high T cell subset regulates TNF-mediated chronic murine ileitis. J Immunol. 2008; 180:2573–2580. [PubMed: 18250468]
8. Burns RC, Rivera-Nieves J, Moskaluk CA, et al. Antibody blockade of ICAM-1 and VCAM-1 ameliorates inflammation in the SAMP-1/Yit adoptive transfer model of Crohn's disease in mice. Gastroenterology. 2001; 121:1428–1436. [PubMed: 11729122]
9. Bamias G, Martin C, Mishina M, et al. Proinflammatory effects of TH2 cytokines in a murine model of chronic small intestinal inflammation. Gastroenterology. 2005; 128:654–666. [PubMed: 15765401]
10. George TC, Fanning SL, Fitzgeral-Bocarsly P, et al. Quantitative measurement of nuclear translocation events using similarity analysis of multispectral cellular images obtained in flow. J Immunol Methods. 2006; 311:117–129. [PubMed: 16563425]
11. Beum PV, Lindorfer MA, Hall BE, et al. Quantitative analysis of protein co-localization on B cells opsonized with rituximab and complement using the ImageStream multispectral imaging flow cytometer. J Immunol Methods. 2006; 317:90–99. [PubMed: 17067631]
12. de la Motte CA, Hascall VC, Drazba J, et al. Mononuclear leukocytes bind to specific hyaluronan structures on colon mucosal smooth muscle cells treated with polyinosinic acid:polycytidylic acid: inter-alpha-trypsin inhibitor is crucial to structure and function. Am J Pathol. 2003; 163:121–133. [PubMed: 12819017]
13. Stuhlmeier KM. Prostaglandin E2: a potent activator of hyaluronan synthase 1 in type-B-synoviocytes. Biochim Biophys Acta. 2007; 1770:121–129. [PubMed: 16904269]
14. Kao JJ. The NF-kappaB inhibitor pyrrolidine dithiocarbamate blocks IL-1beta induced hyaluronan synthase 1 (HAS1) mRNA transcription, pointing at NF-kappaB dependence of the gene HAS1. Exp Gerontol. 2006; 41:641–647. [PubMed: 16723203]
15. Stuhlmeier KM, Pollaschek C. Differential effect of transforming growth factor beta (TGF-beta) on the genes encoding hyaluronan synthases and utilization of the p38 MAPK pathway in TGF-beta-induced hyaluronan synthase 1 activation. J Biol Chem. 2004; 279:8753–8760. [PubMed: 14676202]
16. Bonder CS, Clark SR, Norman MU, et al. Use of CD44 by CD4+ Th1 and Th2 lymphocytes to roll and adhere. Blood. 2006; 107:4798–4806. [PubMed: 16497973]
17. Alho AM, Underhill CB. The hyaluronate receptor is preferentially expressed on proliferating epithelial cells. J Cell Biol. 1989; 108:1557–1565. [PubMed: 2466850]
18. de La Motte CA, Hascall VC, Calabro A, et al. Mononuclear leukocytes preferentially bind via CD44 to hyaluronan on human intestinal mucosal smooth muscle cells after virus infection or treatment with poly(I. C) J Biol Chem. 1999; 274:30747–30755.
19. Siegelman MH, DeGrendele HC, Estess P. Activation and interaction of CD44 and hyaluronan in immunological systems. J Leukoc Biol. 1999; 66:315–321. [PubMed: 10449175]
20. Lesley J, Howes N, Perschl A, et al. Hyaluronan binding function of CD44 is transiently activated on T cells during an in vivo immune response. J Exp Med. 1994; 180:383–387. [PubMed: 7516415]
21. Koopman G, Taher TE, Mazzucchelli I, et al. CD44 isoforms, including the CD44 V3 variant, are expressed on endothelium, suggesting a role for CD44 in the immobilization of growth factors and the regulation of the local immune response. Biochem Biophys Res Commun. 1998; 245:172–176. [PubMed: 9535803]
22. Screaton GR, Bell MV, Jackson DG, et al. Genomic structure of DNA encoding the lymphocyte homing receptor CD44 reveals at least 12 alternatively spliced exons. Proc Natl Acad Sci U S A. 1992; 89:12160–12164. [PubMed: 1465456]
23. Siegelman MH, Stanescu D, Estess P. The CD44-initiated pathway of T-cell extravasation uses VLA-4 but not LFA-1 for firm adhesion. J Clin Invest. 2000; 105:683–691. [PubMed: 10712440]
24. Wittig B, Schwarzler C, Fohr N, et al. Curative treatment of an experimentally induced colitis by a CD44 variant V7-specific antibody. J Immunol. 1998; 161:1069–1073. [PubMed: 9686562]

25. Wittig BM, Johansson B, Zoller M, et al. Abrogation of experimental colitis correlates with increased apoptosis in mice deficient for CD44 variant exon 7 (CD44v7). J Exp Med. 2000; 191:2053–2064. [PubMed: 10859330]

26. Nandi A, Estess P, Siegelman M. Bimolecular complex between rolling and firm adhesion receptors required for cell arrest; CD44 association with VLA-4 in T cell extravasation. Immunity. 2004; 20:455–465. [PubMed: 15084274]

27. Dustin M. A supercode for inflammation. Immunity. 2004; 20:361–362. [PubMed: 15084264]

28. Berlin C, Bargatze RF, Campbell JJ, et al. alpha 4 integrins mediate lymphocyte attachment and rolling under physiologic flow. Cell. 1995; 80:413–422. [PubMed: 7532110]

29. von Andrian UH, Mackay CR. T-cell function and migration. Two sides of the same coin. N Engl J Med. 2000; 343:1020–1034. [PubMed: 11018170]

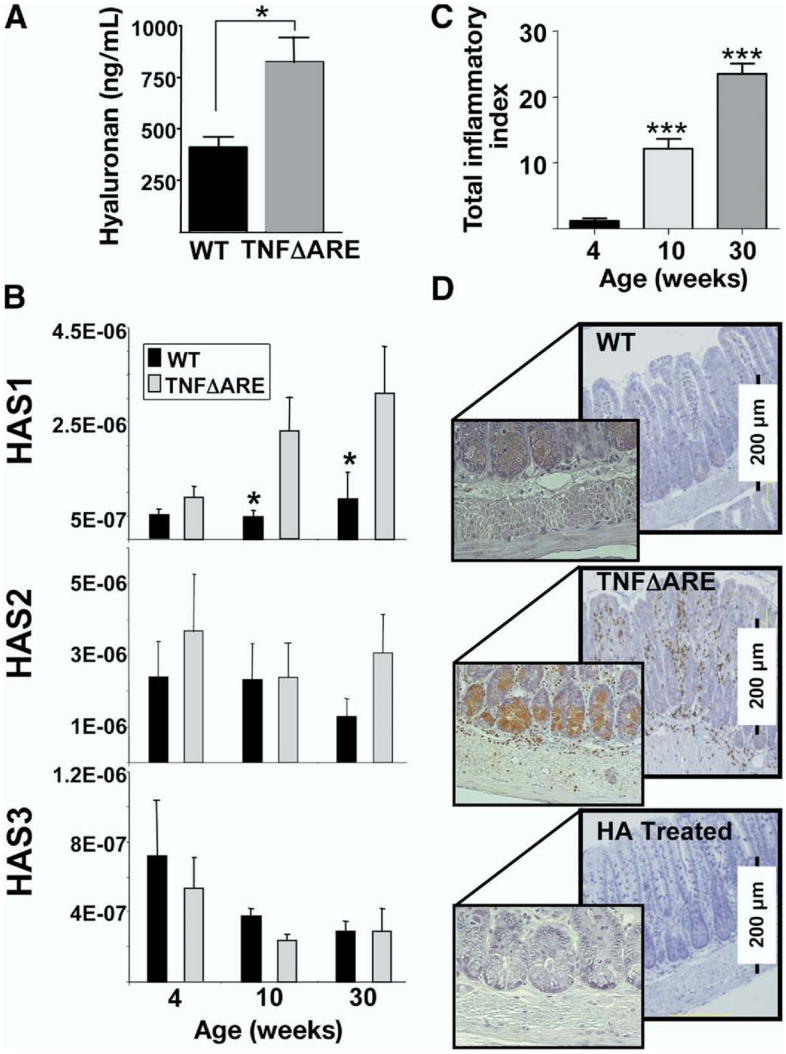

Figure 1.

Serum HA levels and ileal expression of HAS-1 mRNA increased in TNFΔARE mice. (*A*) Levels of HA in serum were determined by enzyme-linked immunosorbent assay (n = 7/strain; **P* < .05). (*B*) mRNA levels for HAS-1, -2, and -3 were determined using real-time reverse-transcription PCR, and normalized to the 18s ribosomal RNA internal control in each sample of ileum of WT (black bars) and TNFΔARE mice (gray bars; n = 10 mice/time point, mean ± SEM; **P* < .05). (*C*) The severity of ileitis was assessed at 4, 10, and 30 weeks of age as described[8] (n = 10 mice/time point, total index represents the sum of individual active, chronic, and transmural indices). (*D*) HA binding protein reactivity localized to infiltrating leukocytes and small intestinal crypts. Pre-incubation with soluble HA inhibited binding of HBP. Representative micrographs are from 3 separate experiments; original magnification, 20×.

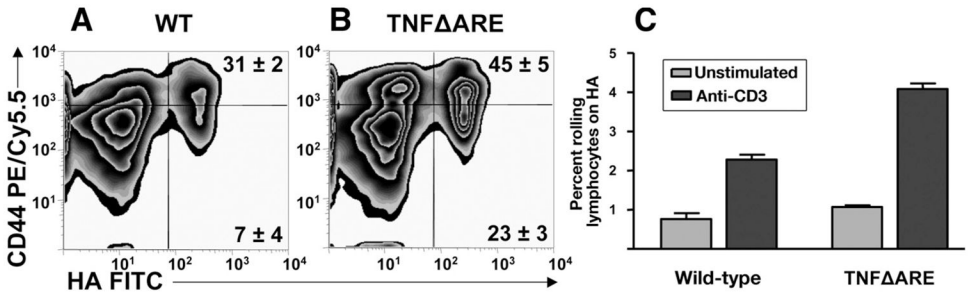

Figure 2.

Enhanced HA binding and rolling flux fraction of $CD4^+$ in TNFΔARE mice. (*A* and *B*) $CD4^+$ T cells from the MLN of TNFΔARE mice and WT littermates were incubated with fluorescein isothiocyanate (FITC)-labeled HA (HA-FITC) and analyzed by flow cytometry. Unconjugated soluble HA was used as specificity control (data not shown). Cells were gated on forward scatter, side scatter, and CD4. Representative data are from 4 mice at 20 weeks of age. (*C*) Physiologic flow conditions were produced using a flow chamber at 2 dyn/cm^2. Rolling interactions were analyzed using 10^7 cells in 8 or more fields of view (pooled mean ± SEM rolling fraction from 3 separate experiments; $P < .05$).

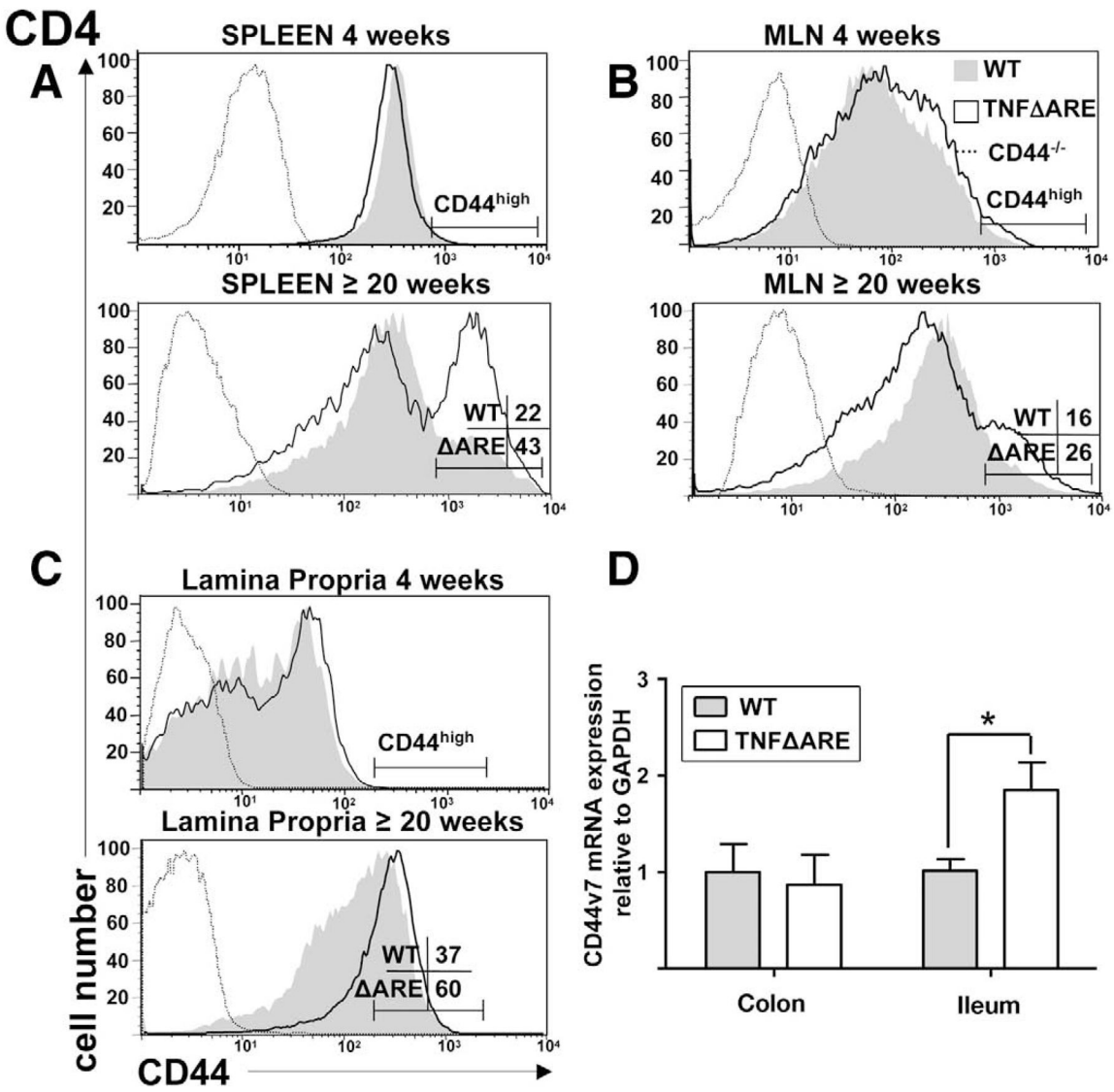

Figure 3.

Expansion of CD44^{high} subset within CD4^{+} T cells with progression of ileitis in indicated compartments of TNFΔARE mice compared with age-matched WT littermates. (*A–C*) Lymphocytes were incubated with anti-CD4, and allophycocyanin- or PE-Cy5.5–labeled anti-CD44 monoclonal antibodies and analyzed by flow cytometry using CD44-deficient lymphocytes (*discontinuous line*) from the respective organs and isotype antibody (MFI < 10^1, not shown) as controls. Cells were gated on forward scatter, side scatter, and indicated populations. Representative histograms obtained from 3–6 mice/group at 4 and 20 or more weeks of age. (*D*) mRNA levels for CD44v7 were determined using real-time reverse-transcription PCR, and normalized to the glyceralde-hyde-3-phosphate dehydrogenase (GAPDH) mRNA internal control in each sample of ileum and colon of WT (*gray bars*) and TNFΔARE mice (*white bars*) at 20 or more weeks of age (n = 10 mice/strain, mean ± SEM; **P* < .05).

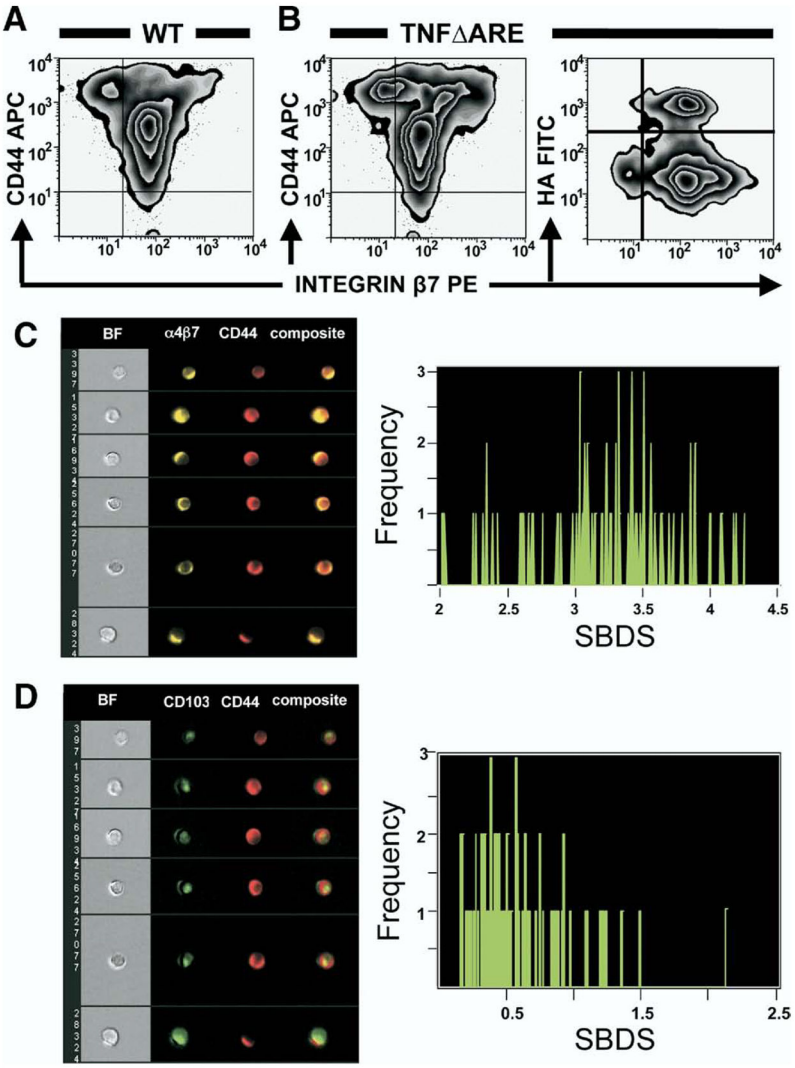

Figure 4.

$CD4^+$ T cells co-expressed integrin β_7 and CD44, which colocalized with integrin $\alpha_4\beta_7$ on the cell surface. (*A* and *B*) Lymphocytes isolated from MLN of TNFΔARE mice and WT siblings were incubated with indicated antibodies and fluorescein isothiocyanate (FITC)-labeled HA, and analyzed by flow cytometry. Cells were gated on forward scatter, side scatter, and CD4 using CD44- and integrin β_7-deficient lymphocytes, and isotype antibodies (MFI < 10^1, not shown) as controls. Representative data were obtained from 4 mice at 20 or more weeks of age run in duplicate. (*C* and *D*) Multispectral imaging flow cytometry suggested colocalization of CD44 and integrin $\alpha_4\beta_7$ on the cell surface but not with CD103, as confirmed by SBDS determination (*right panels*; median ± SEM = 3.3 ± 0.5 vs 0.5 ± 0.4).

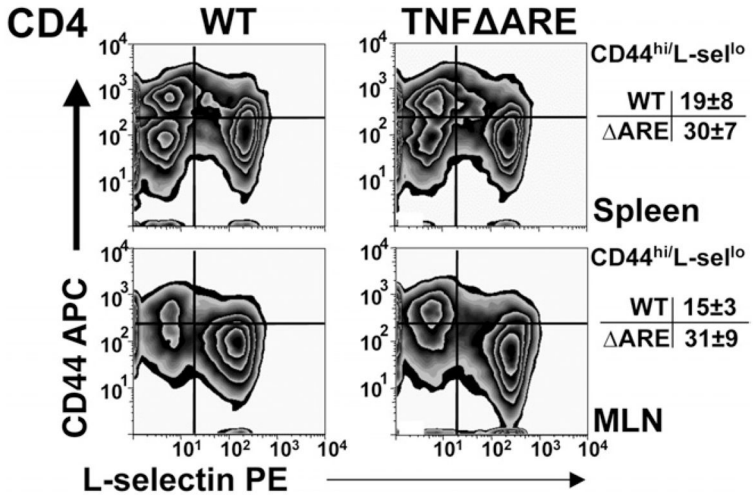

Figure 5.

Expansion of effector $CD4^+$ T cells in TNFΔARE mice. Lymphocytes from indicated compartments were incubated with indicated monoclonal antibodies and analyzed by flow cytometry using CD44- and L-selectin–deficient lymphocytes and isotype antibodies (MFI < 10^1, not shown) as controls. Representative CD44 and L-selectin expression of cells gated on forward scatter, side scatter, and CD4 obtained from 4 mice at 20 or more weeks of age.

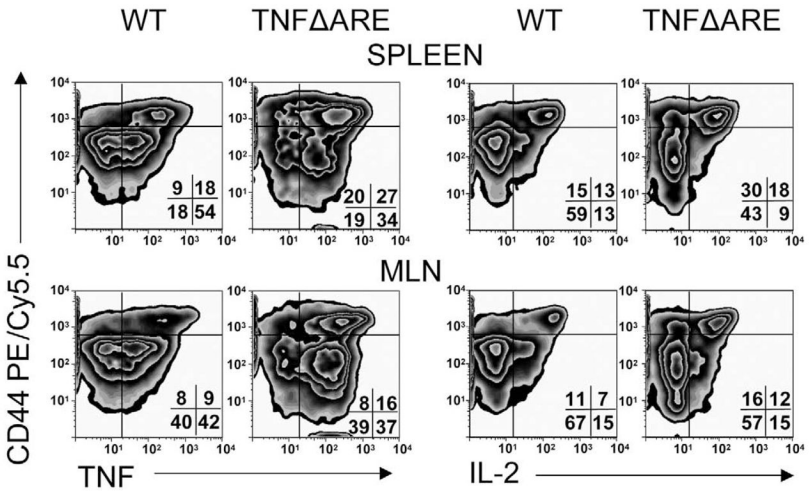

Figure 6.

The proportion of $CD4^{+}/CD44^{high}$ T cells that produce TNF and interleukin (IL)-2 increased in TNFΔARE mice. Lymphocytes from indicated compartments of WT or TNFΔARE mice were stimulated with phorbol myristate acetate/ionomycin, incubated with indicated antibodies, and analyzed by flow cytometry. Cells were gated on forward scatter, side scatter, and CD4 using CD44-deficient lymphocytes for surface staining and isotype antibody for intracellular staining controls (MFI < 10^{1}, not shown). Representative density plots were obtained from 3 experiments using 4 mice per strain at 20 or more weeks of age.

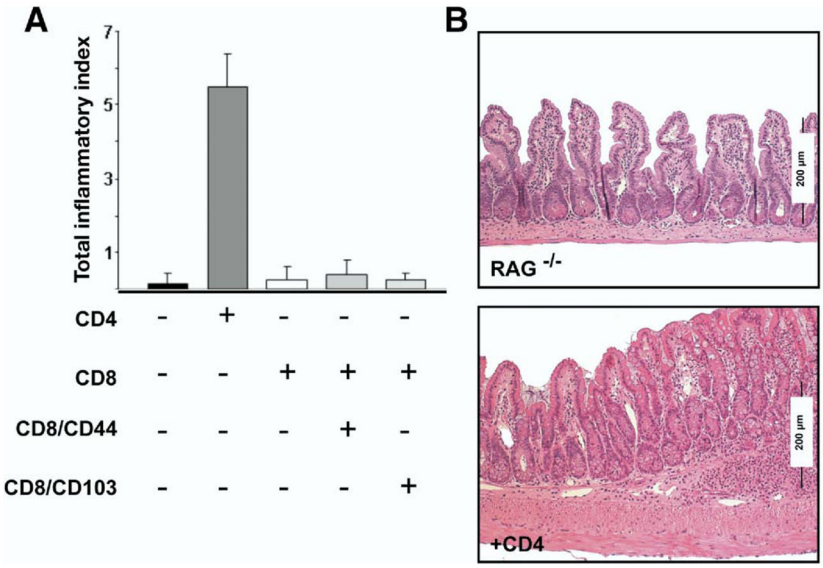

Figure 7.

$CD4^+$ but not $CD8^+$ T cells transfer ileitis to $RAG^{-/-}$ mice. (*A*) $CD4^+$, unfractionated CD8, $CD8/CD44^+$, or $CD8/CD103^+$ cells isolated from spleen and MLN were transferred into $RAG^{-/-}$ mice and the severity of ileitis was assessed after 6 weeks, as described in Burns et al[8] (mean ± SEM from 2 experiments, n = 7/group; $*P < .05$). (*B*) Representative histology of terminal ileum of $RAG^{-/-}$ mice receiving vehicle or $CD4^+$ T cells. Representative micrographs are shown (H&E; original magnification, 10×).

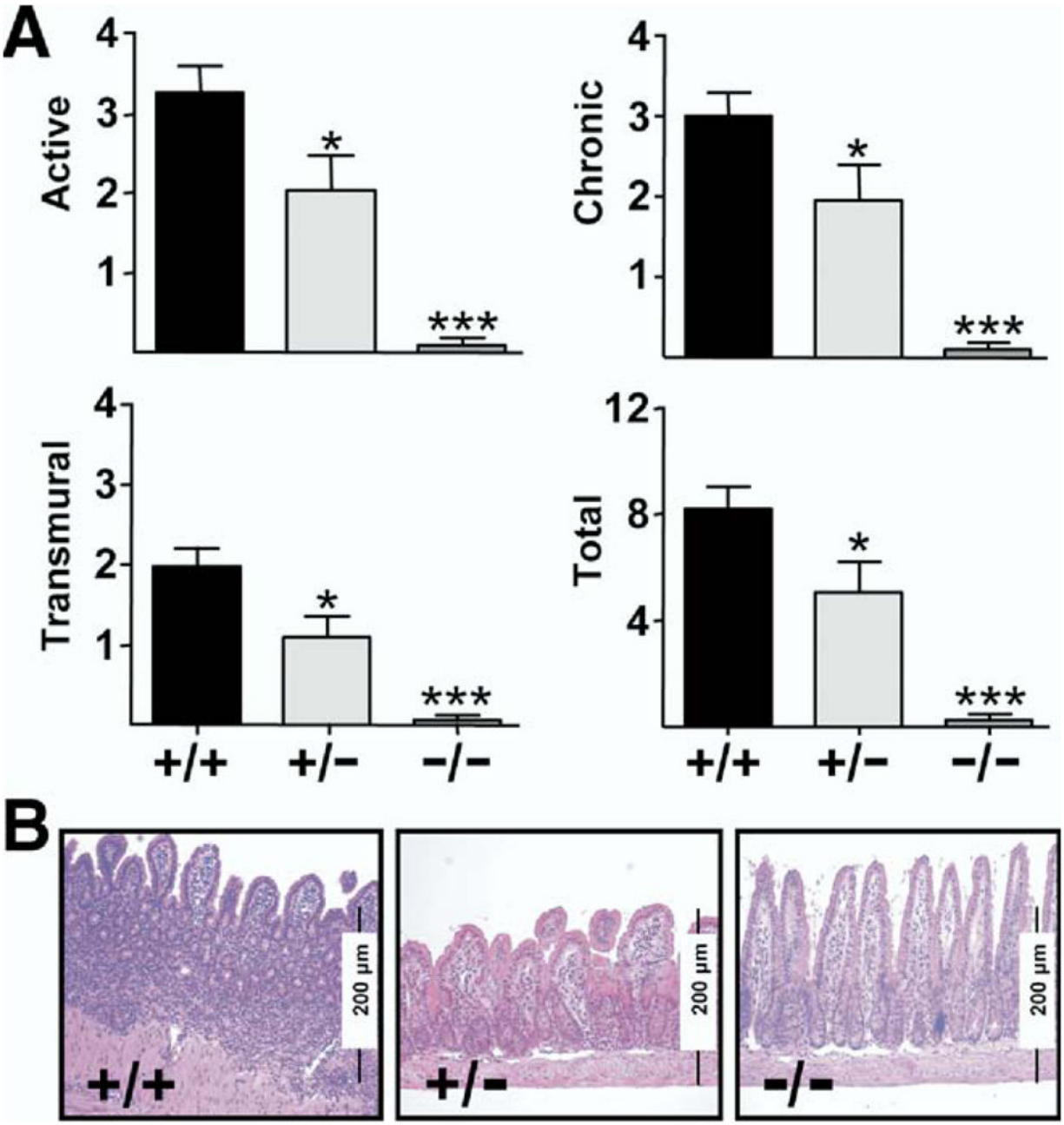

Figure 8.

CD44 deficiency attenuates ileitis. (*A*) Active, chronic, trans-mural, and total inflammatory indices from ilea of 8-week-old CD44-sufficient TNFΔARE mice (+/+; n = 35) were compared with mice heterozygous for CD44 (+/−; n = 21) and CD44-deficient TNFΔARE mice (−/−; n = 16). Attenuation of ileitis correlated with surface expression of CD44. Mean ± SEM, **P* < .05, ****P* < .0001. (*B*) Representative micrographs (H&E; original magnification, 10×).